

Time-Resolved Spectroscopic Studies of B₁₂ Coenzymes: The Photolysis and Geminate Recombination of Adenosylcobalamin

Larry A. Walker II, Joseph J. Shiang, Neil A. Anderson, Stuart H. Pullen, and Roseanne J. Sension*

Contribution from the Department of Chemistry, University of Michigan, Ann Arbor, Michigan 48109-1055

Received March 26, 1998

Abstract: Femtosecond transient absorption spectroscopy has been used to investigate the photolysis of coenzyme B₁₂ (5'-deoxyadenosylcobalamin). Transient kinetic measurements obtained at wavelengths between 400 and 633 nm were analyzed globally to obtain time constants. Transient spectral data obtained for time delays between 5 ps and 9 ns were analyzed by matrix decomposition to identify distinct spectral components present in the data. Photoexcitation results in homolysis of the carbon–cobalt bond forming a singlet radical pair on a picosecond time scale. The subsequent spectral changes probe conformational relaxation and geminate recombination. Analysis of the spectral data suggests that 76 ± 4% of the geminate radical pairs recombine, resulting in a quantum yield of 0.24 ± 0.04 for the formation of solvent separated radicals, in good agreement with literature values of 0.20 ± 0.03 and 0.23 ± 0.04 [Chen, E.; Chance, M. R. *Biochemistry* 1993, 32, 1480–1487]. The geminate recombination of the adenosyl radical with cob(II)alamin occurs biphasically with exponential time constants of 150 ± 20 ps and 0.5 ± 0.2 ns. The effective recombination rate from a single-exponential fit to the data is (0.250 ns)⁻¹ = 4 ns⁻¹.

Introduction

Chemists have long been intrigued by the efficient and highly selective chemical reaction pathways found in enzymatic systems. Since vitamin B₁₂ was first discovered as a treatment for pernicious anemia in the 1920s, both B₁₂-dependent enzymes and the isolated cobalamin coenzymes have been studied extensively.¹ Interest in these enzymes intensified when the crystal structure of coenzyme B₁₂ was solved, highlighting the presence of a novel carbon–cobalt bond. The B₁₂-dependent enzymes may be classified into two broad categories, methyltransferase enzymes and mutase enzymes. In cobalamin dependent mutase enzymes adenosylcobalamin (coenzyme B₁₂) catalyzes radical rearrangement reactions. The coenzyme B₁₂ contains an approximately octahedral ligation structure around a centrally located cobalt atom. The cobalt is ligated to five nitrogens and one carbon. A corrin ring system, composed of four pyrrole groups, provides four of the nitrogen ligands. In free cobalamin an axially oriented dimethylbenzimidazole provides the fifth nitrogen ligand. The differentiating component in cobalamin is the sixth ligand. For coenzyme B₁₂ this group is 5'-deoxyadenosyl resulting in the formation of adenosylcobalamin. The B₁₂-dependent methyltransferase enzymes bind methylcobalamin, where the sixth ligand is a methyl group.

The initial step in the cobalamin dependent reactions in both methyltransferase and mutase enzymes involves breaking the Co(III)–C bond. In methyltransferase enzymes (e.g. methionine synthase) the bond cleavage is heterolytic in which both bonding electrons remain with the cobalt forming a Co(I) species.² In mutase enzymes (e.g. glutamate mutase, methylmalonyl-CoA mutase) the cleavage is homolytic, producing a Co(II) species.³

An important, but as yet unanswered, question in B₁₂ chemistry is how carbon–cobalt bond reactivity can be directed so differently in the methyl- and adenosylcobalamin coenzymes. A solid understanding of B₁₂ catalysis will require detailed knowledge of the factors which influence both the relative energies of the possible bond-cleavage products and the pathways available for cleavage.

It has long been known that photolysis of methylcobalamin and adenosylcobalamin in free solution results in homolytic cleavage of the carbon–cobalt bond with a substantial quantum yield.^{4,5} Continuous wave measurements, with excitation at 442 nm, determined quantum yields of $\phi = 0.20 \pm 0.03$ for adenosylcobalamin and $\phi = 0.35 \pm 0.03$ for methylcobalamin.⁶ Although photolysis might be considered as a model for thermolysis in the study of enzyme mechanism, the validity of such a comparison has been questioned, especially in the absence of a detailed understanding of the photolysis mechanism.^{7–9} On the other hand, an enormous understanding has been afforded by extensive photodissociation studies of ligated porphyrins in both enzyme-bound and free solution. Detailed studies of B₁₂ systems should prove equally fruitful.

A few time-resolved studies of cobalamin photolysis are reported in the literature. An early study of adenosylcobalamin revealed a nanosecond recovery in the transient absorption signal assigned to geminate recombination of the carbon–cobalt bond of sufficient magnitude to account for the observed photolysis

(4) Hogenkamp, H. P. C. In *B₁₂*; Dolphin, D., Ed.; John Wiley and Sons: New York, 1982; Vol. 1, pp 295–323.

(5) Pratt, J. M.; Whitear, B. R. D. *J. Chem. Soc. A* 1971, 252–255.

(6) Chen, E.; Chance, M. R. *Biochemistry* 1993, 32, 1480–1487.

(7) Finke, R. G. In *Molecular Mechanisms in Bioorganic Processes*; Bleasdale, C., Golding, B. T., Eds.; The Royal Society of Chemistry: Cambridge, 1990.

(8) Garr, C. D.; Finke, R. G. *Inorg. Chem.* 1993, 32, 4414–4421.

(9) Natarajan, E.; Grissom, C. B. *Photochem. Photobiol.* 1996, 64, 286–295.

* To whom correspondence should be addressed.

(1) Folkers, K. In *B₁₂*; Dolphin, D., Ed.; John Wiley and Sons: New York, 1982; Vol. 1, pp 1–15.

(2) Banerjee, R. V.; Matthews, R. G. *FASEB J.* 1990, 4, 1450–1459.

(3) Marsh, E. N. G. *BioEssays* 1995, 17, 431–441.

yield.¹⁰ The geminate recombination rate deduced from these data was a rather imprecise (1.3 ± 1.1) ns⁻¹. Data on methylcobalamin were insufficient to determine whether a similar recombination occurred following photolysis. Recent measurements by Grissom and co-workers provide a more accurate estimate of the geminate recombination rate in adenosylcobalamin.¹¹ These workers used picosecond resolved spectral measurements around 470 nm to obtain a geminate recombination rate of (1.1 ± 0.06) ns⁻¹ in aqueous solution. Measurements on methylcobalamin indicated little if any geminate recombination.¹² The planar nature of the methyl radical was invoked as the most likely explanation for the lack of geminate recombination in the radical pair following photolysis of methylcobalamin. Nanosecond transient absorption spectra obtained by Chen and Chance demonstrated that the photoproduct present 10 ns after photolysis of adenosylcobalamin is spectroscopically identifiable as the cob(II)alamin photoproduct with a quantum yield of 0.23 ± 0.04 .¹³ No other photoproduct is observed. Both Chance and Grissom also observed additional diffusive recombination on a much longer microsecond time scale.^{12,13}

In the present series of investigations time-resolved studies of the bond photolysis are used to investigate the reactivity of the carbon–cobalt bond in alkylcobalamins. We have recently reported the results of a spectroscopic study of the primary photochemistry of methylcobalamin.¹⁴ When excited at 400 nm, 27% of the initially excited methylcobalamin undergoes a bond homolysis on a subpicosecond time scale. The remaining 73% forms a metastable photoproduct with a spectrum reminiscent of cob(III)alamin compounds. The spectrum of the metastable photoproduct exhibits a prominent γ band at 340 nm, characteristic of a cob(III)alamin with a very weak axial ligand. These data suggest that the metastable photoproduct might be an ion pair formed following heterolytic cleavage of the carbon–cobalt bond to five-coordinate cob(III)alamin and a methyl anion. The metastable photoproduct recovers to the ground electronic state of methylcobalamin on a 1.2 ± 0.5 ns time scale, leaving only cob(II)alamin observed at 9 ns. The primary photochemical yield of cob(II)alamin is determined largely by the branching ratio between the two photoproduct channels. No geminate recombination of cob(II)alamin and methyl radical is observed.

The present paper reports a complementary investigation of the primary photochemistry and geminate recombination of adenosylcobalamin following excitation at 400 nm. The results reported here lend support for the use of photolysis as a model for thermolysis in the study of coenzyme B₁₂ dependent mutase enzymes. Photoexcitation results in homolysis of the carbon–cobalt bond forming a singlet radical pair on a picosecond time scale. The subsequent spectral changes probe conformational relaxation and geminate recombination. Analysis of the spectral data suggests that $76 \pm 4\%$ of the geminate radical pairs recombine, resulting in a quantum yield of 0.24 ± 0.04 for the formation of solvent-separated radicals, in good agreement with literature values of 0.20 ± 0.03 ⁶ and 0.23 ± 0.04 .¹³ The geminate recombination of the adenosyl radical with cob(II)alamin occurs biphasically with exponential time constants of 150 ± 20 ps and 0.5 ± 0.2 ns.

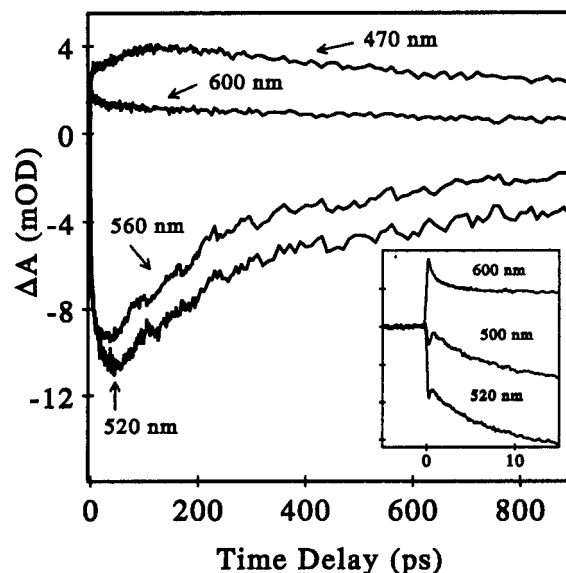


Figure 1. Transient absorption kinetics observed following femtosecond excitation at 400 nm. The probe wavelengths are indicated. The inset highlights the very early kinetic components.

Experimental Section

Transient absorption measurements on adenosylcobalamin were performed with use of a regeneratively amplified femtosecond Titanium Sapphire laser system as described in detail previously.^{14,15} Isotropic kinetic data were obtained by rotating the polarization of the pump beam to magic angle (54.7°) with respect to the polarization of the probe beam, or were constructed from individual parallel and perpendicularly polarized kinetic traces as:

$$I_{\text{iso}}(t) = \langle \frac{1}{3} \rangle [I_{\parallel}(t) + 2I_{\perp}(t)] \quad (1)$$

In addition, the transient anisotropies were constructed from the individual parallel and perpendicularly polarized kinetic traces as:

$$r(t) = \frac{I_{\parallel}(t) - I_{\perp}(t)}{I_{\parallel}(t) + 2I_{\perp}(t)} \quad (2)$$

Calculated in this fashion, the anisotropy is a measure of the average angle ($\theta(t)$) between the pumped and probed transition dipoles:

$$r(t) = 0.4 \langle P_2(\cos\theta(t)) \rangle \quad (3)$$

where P_2 is the second Legendre polynomial.

Adenosylcobalamin was obtained from Sigma and used without further purification. The samples were prepared and kept under anaerobic conditions. This was done by bubbling argon through double distilled deionized water for a minimum of 1 h after which ca. 2 mM solutions were made. The samples were placed in a reservoir and kept under argon. The reservoir was placed in an ice bath to prevent thermal degradation. The samples were flowed through a 1 mm path length cell with a rate sufficient to ensure that the sample volume was refreshed between pulses. The adenosylcobalamin samples had a pH of 6.82 and were not buffered. UV–visible spectra of the sample obtained before and after laser exposure were the same. A steady state difference spectrum for the formation of cob(II)alamin from adenosylcobalamin was obtained as described previously for methylcobalamin.¹⁴

Results

Transient Absorption Data. Kinetic data over a 900 ps window were obtained at 470, 520, 540, 560, and 600 nm (Figure 1). Additional data over a time window of 100 ps were

(10) Endicott, J. F.; Netzel, T. L. *J. Am. Chem. Soc.* **1979**, *101*, 4000–4002.

(11) Chagovetz, A. M.; Grissom, C. B. *J. Am. Chem. Soc.* **1993**, *115*, 12152–12157.

(12) Lott, W. B.; Chagovetz, A. M.; Grissom, C. B. *J. Am. Chem. Soc.* **1995**, *117*, 12194–12201.

(13) Chen, E.; Chance, M. R. *J. Bio. Chem.* **1990**, *265*, 12987–12994.

(14) Walker, L. A., II; Jarrett, J. T.; Anderson, N. A.; Pullen, S.; Matthews, R. G.; Sension, R. J. *J. Am. Chem. Soc.* **1998**, *120*, 3597–3603.

(15) Pullen, S.; Walker, L. A., II; Sension, R. J. *J. Chem. Phys.* **1995**, *103*, 7877–86.

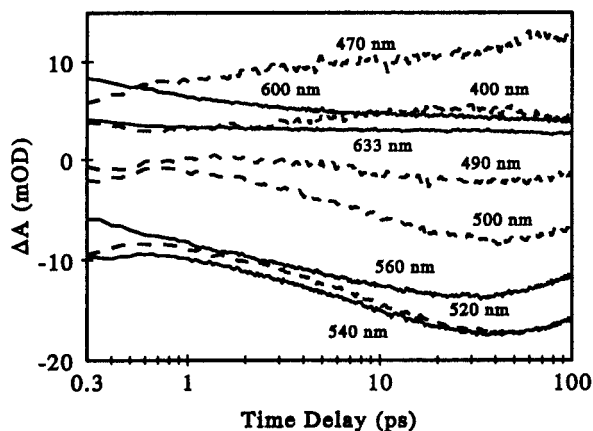


Figure 2. Early visible transient absorption kinetics observed following femtosecond excitation at 400 nm. The logarithmic time scale was chosen to emphasize the variety of kinetic components observed between 500 fs and 100 ps. The probe wavelengths are indicated with wavelengths longer than 525 nm shown as solid lines and wavelengths shorter than 525 nm shown as dashed lines.

obtained at 400, 490, 500, 570, and 633 nm as shown in Figure 2. The latter data traces allowed the recreation of the transient spectral evolution from 0.5 to 100 ps. The transient kinetic data were fitted to a sum of exponentials. Fitting was carried out by subjecting the data to a global analysis, which required the inclusion of 5 decay components and a nondecaying component. The 470 nm data trace required an additional decay component to properly fit the large growth observed in the signal. Optimization of the fitting parameters was carried out by using a simplex algorithm,¹⁶ under the assumption that only the amplitudes, not the rate constants, should be wavelength dependent. The fastest time constant (≤ 0.1 ps) reflects internal conversion and/or bond breaking. The data also required two components associated with bleach increases (time constants of 1.9 ± 0.5 and 17.2 ± 0.5 ps) and two components with large decreasing amplitudes (time constants of 150 ± 20 ps and 0.5 ± 0.2 ns). The longer component is not well defined by the present kinetic traces which only extend to 900 ps, limited by the length of the available optical delay line.

In addition to the magic angle kinetic data described above, the absorption anisotropy was measured for the first 100 ps at a range of wavelengths as shown in Figure 3. The most notable feature in these data is its time independence for delay times longer than a few picoseconds. While the isotropic signal exhibits large-amplitude changes (Figure 2), the anisotropy is quite flat. This observation demonstrates that the kinetic components observed in the isotropic data correlate with little or no change in transition dipole moment.

It is difficult to assign the time constants obtained in the global analysis to specific physical processes without more information on the overall spectral evolution. To further facilitate data analysis, transient absorption difference spectra were obtained every 2.5 ps between 5 and 20 ps and for 9 time delays between 40 ps and 9 ns. The evolution of the difference spectrum is illustrated by the data shown in Figures 4 and 5. The evolution from 0.5 to 20 ps is characterized primarily by an increase in the intensity of the difference spectrum, with little change in spectral shape. The evolution from 40 ps to 9 ns is characterized by a large decrease in the intensity, consistent with the earlier measurements.^{10–12} A modest change in spectral shape is also

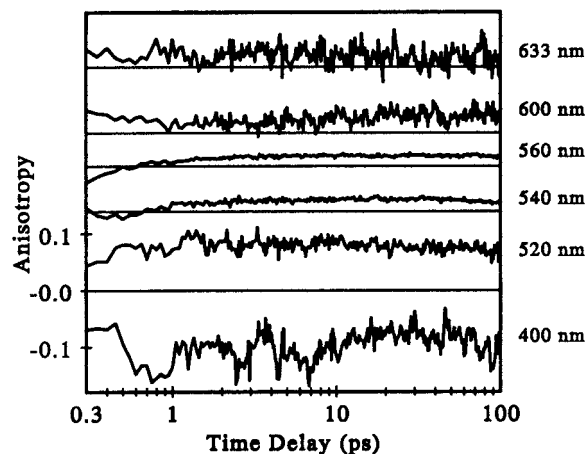


Figure 3. Polarization anisotropy constructed from parallel and perpendicular polarized transient absorption measurements at the indicated wavelengths. Note that the time axis is logarithmic. The 520 and 400 nm traces are plotted according to the scale to the left. The remaining traces are offset vertically for clarity with zero indicated by the parallel lines. Some significant changes in anisotropy are observed over the first two picoseconds. For longer times the anisotropy at each wavelength is essentially constant.

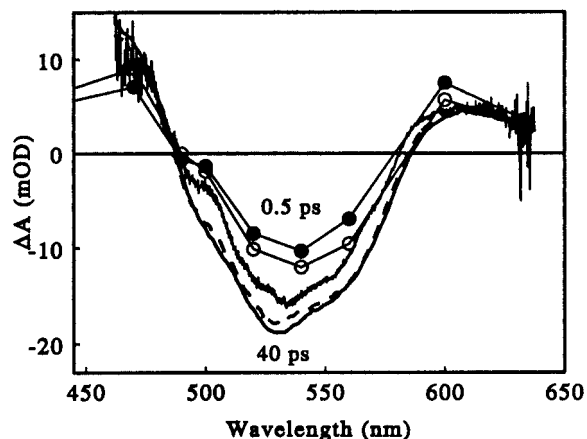


Figure 4. Evolution of the transient difference spectrum following excitation of adenosylcobalamin from 0.5 to 40 ps. Transient absorption difference spectra are plotted for 5 (solid line), 20 (dashed line) and 40 ps (labeled solid line). These data were obtained by using a broad band continuum and a CCD camera. The difference spectra at 0.5 (filled circles) and 2.0 ps (open circles) were obtained from the kinetic behavior observed at specific wavelengths (as shown in Figure 2).

apparent between 40 and 350 ps, with the largest change observed near the cob(II)alamin peak absorption at 470 nm. This is highlighted by the comparison in the inset to Figure 5. The difference spectra shown for 900 ps and 9 ns following excitation of adenosylcobalamin are entirely consistent with the formation of cob(II)alamin as expected from steady state and nanosecond measurements.^{4–6,13}

From the data discussed above, it is apparent that a transient absorption measurement at any single wavelength is unlikely to yield an accurate description of the geminate recombination kinetics between cob(II)alamin and the adenosyl radical. This is particularly true near the cob(II)alamin peak at 470 nm where the slow rise in the peak intensity results in an apparent small-amplitude, slow decay. The intensity of the overall difference spectrum decays much more rapidly. To obtain an accurate picture of the overall decay of the signal, the integrated spectral intensity in the difference spectrum as a function of time is plotted in Figure 6. These data exhibit a large increase in the intensity during the first 50 ps, followed by a decay to a plateau

(16) Press: W. H.; Teukolsky, S. A.; Vetterling, W. T.; Flannery, B. P. *Numerical Recipes in C: The art of scientific computing*, 2nd ed.; Cambridge University Press: New York, 1992.

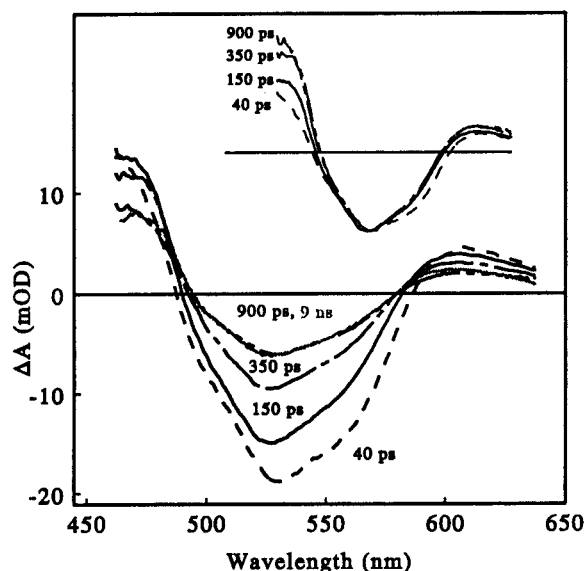


Figure 5. Evolution of the transient difference spectrum from 40 ps to 9 ns following excitation of adenosylcobalamin. The inset shows the spectra between 40 and 900 ps scaled to the same bleach intensity to highlight the spectral changes. For time delays of 150 ps and longer the only significant change is around 470 nm.

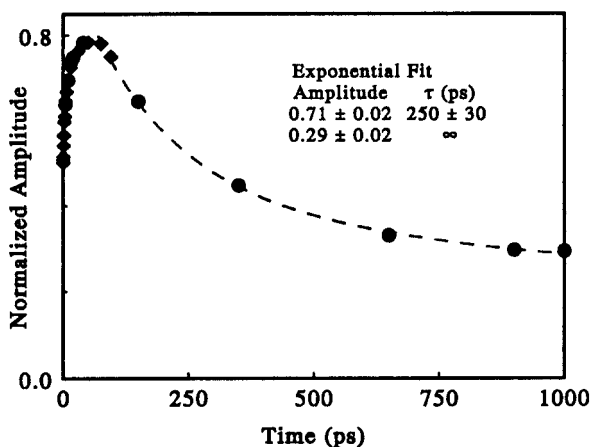


Figure 6. Integrated intensity of the difference spectrum as a function of time after excitation at 400 nm. Diamonds: Integrated intensity deduced from the kinetic measurements between 0.5 and 100 ps. Circles: Integrated intensity obtained from the transient spectral measurements between 5 ps and 1 ns. The dashed line is an exponential fit to the decay as discussed in the text, with parameters listed in the figure.

at longer times. An exponential fit to the decay is shown as the dashed line in Figure 6, with parameters given in the figure. The overall decay of the transient bleaching signal suggests that $71 \pm 2\%$ of the photoproduct returns to the ground state on a time scale of 250 ps while $29 \pm 2\%$ forms solvent-separated radical pairs. Assuming that cob(II)alamin is produced with unit quantum yield within 40 ps and that only one species contributes to the difference spectrum, this transient absorption data suggests a quantum yield for photoproduct formation of 0.29 ± 0.02 , in reasonable agreement with the value of 0.23 ± 0.04 obtained by Chen and Chance from nanosecond measurements.⁶ The agreement is better if the primary quantum yield for photolysis is somewhat less than unity.

The global analysis of the transient absorption data suggests that the geminate recombination of cob(II)alamin and adenosyl radical is actually biexponential rather than single exponential. Analysis of the data according to a biexponential decay model

yields the following amplitudes for the decay components: 0.30 ± 0.10 (150 ± 20 ps); 0.46 ± 0.10 (0.5 ± 0.2 ns); and 0.24 ± 0.04 (solvent-separated radical pairs). The quantum yield of 0.24 ± 0.04 obtained from the biexponential fit is in excellent agreement with the nanosecond quantum yield obtained by Chen and Chance.⁶

Singular Value Decomposition Analysis. The difference spectra obtained between 20 ps and 9 ns were subjected to analysis by using a singular value decomposition (SVD) algorithm:¹⁷

$$\mathbf{A} = \mathbf{U} \cdot \mathbf{S} \cdot \mathbf{V}^T \quad (4)$$

where \mathbf{A} is the data matrix containing the transient difference spectra as a function of wavelength and time. This matrix is decomposed into \mathbf{U} , a matrix of the basis spectra, \mathbf{S} , a diagonal matrix containing the singular values, and \mathbf{V}^T , a matrix containing basis population vectors.

By comparing the singular values and analyzing the auto-correlations of each of the spectral basis vectors, it was determined that only two of the spectral basis vectors contained signal while the remaining vectors were predominantly noise. Therefore, the transient difference spectra are dominated by the presence of two species of varying population. Only these two basis vectors are retained for further analysis.

Discussion

Derivation of Species Associated Difference Spectra. In conjunction with a kinetic model for the data, the results of the SVD analysis may be used to construct species associated difference spectra from the two significant spectral basis vectors. First, decay associated difference spectra are derived from the basis spectra obtained from SVD analysis as follows:

$$\mathbf{F} = \mathbf{U}' \mathbf{P}^T \quad (5)$$

where \mathbf{F} contains the decay associated difference spectra, \mathbf{P} is a parameter matrix, and $\mathbf{U}' = \mathbf{U}\mathbf{S}$ is the product of the spectral basis vectors and their corresponding singular values. The parameters contained within the 2×2 \mathbf{P} matrix were optimized with the constraint that one of the species present is cob(II)alamin. This is a reasonable constraint based on the comparison of the transient difference spectra obtained for time delays longer than 350 ps with the steady state difference spectrum for the formation of cob(II)alamin (See Figure 7). The amplitude as a function of time for each decay associated spectrum (\mathbf{C}) is given by:

$$\mathbf{C} = \mathbf{V} \mathbf{P}^{-1} \quad (6)$$

where \mathbf{V} contains the two basis vectors retained from the SVD analysis. The decay associated spectra and relative amplitudes as a function of time are plotted in Figure 7. The difference spectrum which corresponds to all of the amplitude for time delays between 650 ps and 9 ns is also compared with the steady state difference spectrum of cob(II)alamin in Figure 7. Clearly, the only cobalamin species present at long times is spectroscopically identifiable as cob(II)alamin.

So far, two assumptions have been made in the data analysis: First, only two distinct species contribute to the transient absorption spectrum after 40 ps. This assumption is based on a comparison of the singular values and on the autocorrelation of the basis spectra obtained in the SVD

(17) Henry, E. R.; Hofrichter, J. *Methods Enzymol.* **1992**, *210*, 129–192.

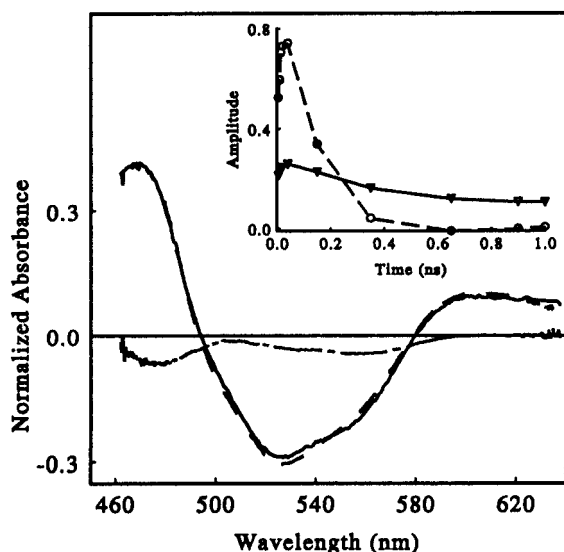


Figure 7. Decay associated spectra obtained from an SVD analysis of the data between 20 ps and 9 ns. The solid line is the steady-state cob(II)alamin spectrum, while the dashed line is the transient cob(II)alamin spectrum. The dot-dashed line is the decay associated spectrum associated with the 130 ps decay component. The inset shows the population behavior of the two decay associated spectra.

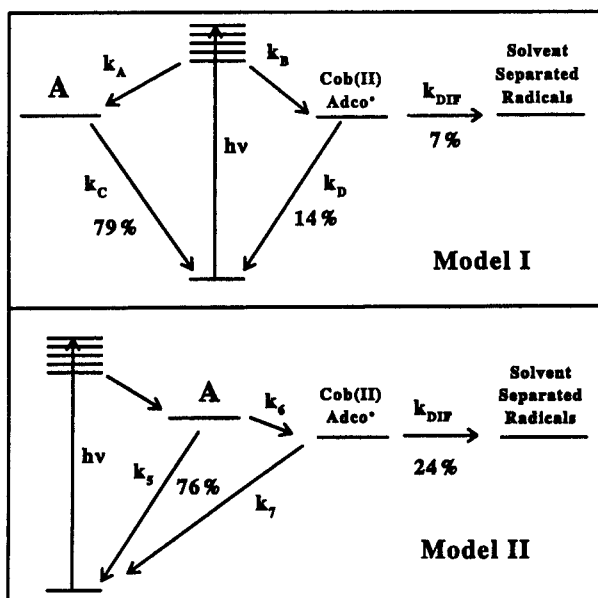


Figure 8. Two models for the photolysis of adenosylcobalamin consistent with the observed kinetic behavior. In Model I, photoexcitation and internal conversion results in a branching between two distinct photoproduct channels on a picosecond time scale. The metastable intermediate (A) recovers to form ground-state adenosylcobalamin on a time scale of ca. 130 ps. The cob(II)alamin and adenosyl radical pairs undergo geminate recombination in competition with diffusion to form solvent-separated radical pairs. In Model II photoexcitation and internal conversion result in the formation of a metastable photoproduct (A) that is an intermediate in the formation of the steady-state cob(II)alamin photoproduct.

decomposition. Second, one of the species is cob(II)alamin. At this point it is necessary to make a third assumption and propose a model for the photochemistry of adenosylcobalamin. Two different models, sketched in Figure 8, may be supported by the picosecond data. Model I assigns the smaller decay associated spectrum to a metastable species similar to the model for photolysis in methylcobalamin.¹⁴ The magnitude of the difference spectrum demands that this species have a spectrum

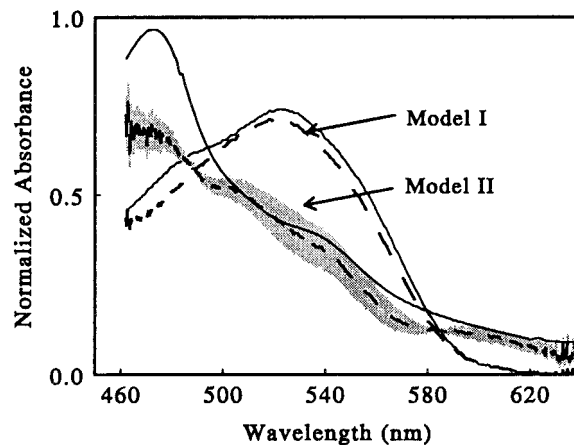


Figure 9. Species associated spectra observed between 5 ps and 9 ns after excitation of adenosylcobalamin at 400 nm. The spectra are obtained by adding the steady-state adenosylcobalamin spectrum to the species associated difference spectrum obtained from the SVD analysis. The dark solid lines are the steady-state spectra of cob(II)alamin and adenosylcobalamin. The dashed lines represent the spectra of the species labeled A in Figure 8. The gray shaded region represents the error bar on the species associated spectrum derived according to Model II. The primary source of error is the uncertainty in the long time constant.

very similar to that of adenosylcobalamin, but slightly weaker across the visible region of the spectrum (Figure 9). If Model I is correct 79% of the initially excited molecules form a metastable intermediate that converts to ground-state adenosylcobalamin on a time scale of ca. 150 ps. The remaining 21% of the excited adenosylcobalamin undergoes bond homolysis with two-thirds of the radical pairs undergoing geminate recombination on a time scale of ca. 500 ps.

There are three primary arguments against this first model. (1) The difference spectrum of the metastable species is nondescript, representing primarily a global decrease in intensity. This is in contrast to the well-defined, structured difference spectrum observed following the excitation of methylcobalamin. (2) The anisotropy behavior seen in Figure 3 would require that the absorption signal due to the metastable state and cob(II)alamin have similar polarization characteristics. While this is not impossible, it is unlikely for two distinct chemical species. (3) Analysis of the data according to Model I implies a quantum yield of 0.07 ± 0.03 for the formation of solvent-separated radical pairs, a factor of 3 lower than the quantum yields determined for excitation at 355, 442, and 532 nm in the careful work of Chen and Chance.^{6,13} This last argument is the most compelling, and taken in conjunction with the other two leads us to dismiss Model I from further consideration.

Model II suggests the presence of an intermediate in the formation of cob(II)alamin, with recombination to the ground state occurring from both the intermediate and the spectroscopically identified cob(II)alamin radical pair. The parameter matrix, \mathbf{P} , is constructed to obtain the best least-squares agreement between calculated populations ($\mathbf{C} = \mathbf{V}\mathbf{P}^{-1}$) and the populations expected from the exponential decays in Model II. This constraint leads to the species associated spectrum labeled Model II in Figure 9. The uncertainty in this spectrum arises from the large uncertainty in the recombination time constant (0.5 ± 0.2 ns). The intermediate species has a broad structureless spectrum resembling that of a cob(II)alamin species—but with much less intensity near the cob(II)alamin peak absorption at 470 nm. This analysis is identical to the biexponential analysis discussed above and implies a quantum yield of 0.24 ± 0.04 for the formation of solvent-separated

radicals in good agreement with literature values of 0.20 ± 0.03^6 and 0.23 ± 0.04 .¹³

Identity of the Intermediate Photoproduct. The most likely model for the photolysis of adenosylcobalamin is that sketched as Model II in Figure 8. This model is consistent with both the picosecond dynamics and the steady state quantum yield for photolysis. In the remaining discussion we will assume that this model correctly describes the photolysis of adenosylcobalamin. The species associated spectrum of the intermediate species (labeled A in Figure 8) implied by analysis of the data according to Model II is similar to the spectrum of cob(II)alamin and globally distinct from the spectra observed for cob(I)alamin and cob(III)alamin species.¹⁴ In addition, the absorption anisotropy does not reflect the conversion from the intermediate to cob(II)alamin. It is quite reasonable, therefore, to propose that this species corresponds to conformationally strained cob(II)alamin, formed following homolytic cleavage of the carbon–cobalt bond.

Relaxation of the corrin ring following homolysis of adenosylcobalamin is expected on the basis of X-ray studies that have investigated the structures of adenosylcobalamin, methylcobalamin, and cob(II)alamin. Kratky and co-workers reported the crystal structure of cob(II)alamin and its variation from both adenosylcobalamin and methylcobalamin.¹⁸ No identifiable changes in the bond lengths between the equatorial nitrogens and the cobalt were observed. However, the upward folding of the corrin ring is much more pronounced for methylcobalamin (15.8°) than adenosylcobalamin (13.3°). In addition, while the Co(III) in both of the coenzymes lies in the plane of the equatorial nitrogens within experimental error, the Co(II) in cob(II)alamin is displaced out of the plane, toward the axial nitrogen by 0.12 Å. This out-of-plane motion of the cobalt alters the “upward folding” of the corrin ring to 16.3° in cob(II)alamin. Kräutler et al. reported further that the cobalt to axial nitrogen distance shortened, from 2.24 Å in adenosylcobalamin or 2.19 Å in methylcobalamin to 2.13 Å upon reduction.¹⁸ Later studies by Chance and co-workers used extended X-ray absorption fine structure (EXAFS) to investigate the structures in solution.^{19,20} Their findings are similar for the nitrogen ligation about the Co, although a much shorter cobalt to axial nitrogen distance of 1.99 Å is reported for cob(II)alamin.¹⁹ In either case, it is evident that the axial cobalt–nitrogen bond strengthens upon reduction, thereby distorting the geometry from the adenosylcobalamin structure. It is also noteworthy that the structural changes are much more severe upon reduction of adenosylcobalamin than methylcobalamin.

Following abrupt photoinduced homolysis of the carbon–cobalt bond, the initially formed cob(II)alamin will relax to the steady-state structure on a time scale no faster than picoseconds. In addition, the visible and near-ultraviolet absorption bands of cobalamin species are dependent upon both the conjugation of the corrin ring and the mixing of cobalt d orbitals with the π orbitals of the corrin ring.²¹ Thus, it is likely that the spectral evolution observed in the transient difference spectra reflects the conformational relaxation of the cob(II)alamin photoproduct. This spectral evolution is not apparent following photolysis of methylcobalamin because the structural changes to the corrin ring are much smaller.

(18) Kräutler, B.; Keller, W.; Kratky, C. *J. Am. Chem. Soc.* **1989**, *111*, 8936–8938.

(19) Sagi, I.; Wirt, M. D.; Chen, E.; Frisbie, S.; Chance, M. R. *J. Am. Chem. Soc.* **1990**, *112*, 8639–44.

(20) Scheuring, E.; Padmakumar, R.; Banerjee, R.; Chance, M. R. *J. Am. Chem. Soc.* **1997**, *119*, 12192–12200.

(21) Giannotti, C. In *B₁₂*; Dolphin, D., Ed.; John Wiley and Sons: New York, 1982; Vol. 1, pp 393–430.

Ultrafast Bond Cleavage. The kinetic measurements presented above contain three fast components: (≤ 100 fs), 1.9 ps, and 17 ps. The fastest component is manifest in the initial spike observed in the kinetic data and represents the largest change in both spectral shape and polarization behavior observed in the transient absorption data. The dynamics convoluted into this component are indistinguishable in the present data set, which is limited by a ca. 300 fs instrument response function. Presumably this fastest component reflects internal conversion from the initially excited electronic state to the lower-lying excited states. Depending on the nature of the excited state potential energy surfaces, bond cleavage could also occur on this time scale. The 1.9 ps component has a relatively small amplitude characterized in general by a ca. 20% increase in the magnitude of the transient difference spectrum and correlates with very small anisotropy changes at a few wavelengths.

To identify spectroscopically distinct components at early times, an SVD analysis of the spectral data obtained between 5 and 40 ps was carried out. This analysis yields only one significant basis spectrum with an amplitude that increases by 25% over this time range. This basis spectrum is identical within error to the species associated spectrum derived from an SVD analysis of the data matrix obtained between 20 ps and 9 ns according to the constraint of Model II. There is no evidence for an additional distinct spectral species between 5 and 40 ps. This is consistent with the relatively flat anisotropy behavior observed for time delays longer than a few picoseconds.

There are two likely interpretations for the data and analysis presented above. (1) Bond cleavage occurs within two picoseconds of excitation. The 17 ps kinetic component represents spectral evolution resulting from the vibrational and conformational relaxation of the cob(II)alamin radical, which must occur following homolysis. If bond cleavage occurs within a few hundred femtoseconds, the 1.9 ps component would also reflect vibrational relaxation. (2) Fifty to eighty percent of the adenosylcobalamin molecules undergo bond cleavage within 2 ps of excitation. The remaining molecules undergo bond homolysis on a slower time scale, resulting in a near unity quantum yield for bond homolysis within 50 ps. Although it is clear from the data that >75% of the molecules that undergo bond homolysis do so within 5 ps of excitation, a precise description of the bond cleavage dynamics will require analysis of a more extensive data set from ca. 50 fs to 20 ps.

Conclusions

This paper presents a transient absorption study of the primary photolysis and geminate recombination of adenosylcobalamin. Although two distinct models for the photolysis of adenosylcobalamin may be consistent with the observed kinetic data, only one of these models is consistent with the literature values for the photolysis quantum yield. A detailed analysis of the data according to Model II shows the presence of an intermediate photoproduct following excitation. This species has a difference spectrum which resembles that of cob(II)alamin and is therefore assigned to the conformationally strained cob(II)alamin radical. Thus, the only species clearly present after 5 ps is spectroscopically identifiable as cob(II)alamin. Ultrafast bond dissociation is consistent with the results of Grissom and co-workers that indicate that bond dissociation occurs from a singlet charge

(22) Kruppa, A. I.; Taraban, M. B.; Leshina, T. V.; Natarajan, E.; Grissom, C. B. *Inorg. Chem.* **1997**, *36*, 758–759.

(23) Schrauzer, G. N.; Lee, L. P.; Sibert, J. W. *J. Am. Chem. Soc.* **1970**, *92*, 2997–3005.

transfer state^{9,22} and inconsistent with earlier proposals that homolysis occurred following internal conversion to a triplet charge transfer state.^{23–25}

The geminate recombination of the adenosyl radical with cob(II)alamin occurs biphasically with exponential time constants of 150 ± 20 ps and 0.5 ± 0.2 ns. The average observed rate of recombination is ca. $(0.25 \text{ ns})^{-1} = 4 \pm 1 \text{ ns}^{-1}$. Previous work by Endicott and Netzel¹⁰ lacked both the spectral resolution and signal-to-noise ratio required to properly describe the recombination rates. Chagovetz and Grissom deduced a significantly smaller recombination rate from integrating the transient absorption signal around 470 nm.¹¹ However, their reported value is consistent with the 470 nm kinetic trace presented here. Analysis of the 470 nm kinetic trace shown in Figure 1 yields an apparent rate constant for geminate recombination of $(1.04 \pm 0.04) \text{ ns}^{-1}$ in excellent agreement with the experimental result of Chagovetz and Grissom, $(1.1 \pm 0.06) \text{ ns}^{-1}$. In fact the data of Chagovetz and Grissom are entirely consistent with the data and analysis presented here. This result highlights the intrinsic danger present in the use of narrow isolated spectral regions or single wavelengths in the interpreta-

tion of dynamic behavior on the subnanosecond time scale. Vibrational and conformational relaxation processes frequently influence the apparent dynamics in a complex fashion. Ironically, the largest effect, as seen here, is often at the peak of an absorption band. This is the very spectral region usually thought, on longer time scales, to provide the cleanest measure of the population dynamics.

The transient absorption study reported here lends support for the use of photolysis as a model for thermolysis in the study of coenzyme B₁₂ dependent mutase enzymes. Photoexcitation results in homolysis of the carbon–cobalt bond forming a singlet radical pair on a time scale certainly less than 20 ps and probably less than 2 ps. The subsequent spectral changes probe conformational relaxation and geminate recombination. Spectral studies of geminate recombination in enzyme bound coenzyme B₁₂ should provide a useful probe of environmental effects on the C–Co bond strength.

Acknowledgment. We thank Dr. Joseph Jarrett for supplying the steady state spectrum of cob(II)alamin and the cob(II)-alamin–adenosylcobalamin difference spectrum. S.H.P. was supported by the Center for Ultrafast Optical Sciences (NSF-STC-PHY-8920108)

(24) Rao, D. N. R.; Symons, M. C. R. *J. Chem. Soc., Chem. Commun.* **1982**, 954–955.

(25) Sakaguchi, Y. H.; Hayashi, H.; I'Haya, Y. *J. Phys. Chem.* **1990**, *94*, 291–293.